

Investigation of plasma polymerized pyrrole under various gas flow rates and input power using atmospheric pressure plasma jets

Dong Ha Kim, Choon-Sang Park, Won Hyun Kim, Jung Goo Hong, Bhum Jae Shin, Tae Seon Park & Heung-Sik Tae

To cite this article: Dong Ha Kim, Choon-Sang Park, Won Hyun Kim, Jung Goo Hong, Bhum Jae Shin, Tae Seon Park & Heung-Sik Tae (2017) Investigation of plasma polymerized pyrrole under various gas flow rates and input power using atmospheric pressure plasma jets, *Molecular Crystals and Liquid Crystals*, 651:1, 26-34, DOI: [10.1080/15421406.2017.1338489](https://doi.org/10.1080/15421406.2017.1338489)

To link to this article: <https://doi.org/10.1080/15421406.2017.1338489>



Published online: 12 Oct 2017.



Submit your article to this journal [↗](#)



Article views: 40



View related articles [↗](#)



View Crossmark data [↗](#)



Investigation of plasma polymerized pyrrole under various gas flow rates and input power using atmospheric pressure plasma jets

Dong Ha Kim^{a,†}, Choon-Sang Park^{a,†}, Won Hyun Kim^b, Jung Goo Hong^b, Bhum Jae Shin^c, Tae Seon Park^b, and Heung-Sik Tae^a

^aSchool of Electronics Engineering, College of IT Engineering, Kyungpook National University, Daegu, South Korea; ^bSchool of Mechanical Engineering, College of Engineering, Kyungpook National University, Daegu, Korea; ^cDepartment of Electronics Engineering, Sejong University, Seoul, South Korea

ABSTRACT



This paper has investigated the synthesis of plasma-polymerized pyrrole (pPPy) nano-particles grown by the proposed atmospheric pressure plasma jets (APPJs) through the parametric studies, especially input power and gas flow rate. The transition of conventional streamer-like into intense and glow-like discharges necessary for fully cracking the monomer was observed to be strongly dependent on both input power and gas flow rate. The intense and glow-like discharge was produced only when adopting the specific parametric condition, *i.e.*, a gas flow rate of 1600 sccm and input power with 12.5 kV, thereby resulting in obtaining the synthesized pPPy nano-particle structures with highly cross-linked networks and many double bonds. The plasma-flow characteristics were investigated based on the non-plasma flow numerical simulation, and also analyzed by the voltage, current, infrared, and optical emission spectroscopy (OES). The synthesized pPPy films were analyzed by field-emission scanning electron microscopy (FE-SEM) and Fourier infrared spectroscopy (FT-IR). It is anticipated that the high-quality plasma polymer grown by the proposed APPJs contributes to serving as conducting electrode-materials of a flexible polymer light emitting diode (P-LED).

KEYWORDS

Atmospheric pressure plasma polymerization; pyrrole; conducting polymer; numerical theory; electrode-material

1. Introduction

Since the first successful synthesis of the conducting polymer was reported [1], the conducting polymer having high flexibility and conductivity feature has widely been studied for applications in a variety of industrial fields such as display, gas sensor, and nano-electronic devices [2–5]. Among various applications, flexible electrode-materials of stretchable display have gained much attention since the first polymer light emitting diode (P-LED) device was invented [6]. However, almost all the electro-active polymers such as polypyrrole, polythiophene, and polyaniline were polymerized by solution/wet processes with high growth temperature (100~300 °C), which could damage the heat-sensitive substrates. Whereas, the atmospheric pressure plasma (APP) polymerization system enables dry and room-temperature

CONTACT Heung-Sik Tae  hstae@ee.knu.ac.kr  School of Electronics Engineering, College of IT Engineering, Kyungpook National University, Daegu 702-701, South Korea

[†]These authors contributed equally to this work.

Color versions of one or more of the figures in the article can be found online at www.tandfonline.com/gmcl.

processes for synthesizing plasma polymer films with electrical conductivity, which would be suitable for employing a wide range of substrates without thermal damages on substrates [7, 8]. Furthermore, plasma polymers are known to be branched, highly cross-linked, insoluble, pinhole-free, and adhere well to most substrates [9, 10]. Park et al. reported a new polymer synthesis technique using novel atmospheric pressure plasma jets (APPJs) adopting additional glass tube and PTFE bottom holder. The previous results have shown that the new APPJs device, where the PTFE bottom holder was located within the glass tube, enabled the high crystalline plasma-polymerized aniline (pPANI) and pyrrole (pPPy) nano-materials to be successfully grown under argon (Ar) dominant gas condition by simply shielding the plasma generation region from the ambient air [11, 12]. In addition, Kim et al. showed that unique plasma characteristics produced in nucleation region of advanced APPJs, i.e., streamer-like or glow-like discharge, could vary considerably depending on the positions of PTFE bottom holder with respect to additional glass tube [13]. Nonetheless, the physics of the plasma have not yet been studied numerically and systematically in terms of the effects of the process parameters such as gas flow rates and input power, where the PTFE bottom holder is located exactly at the end of the glass tube. In this paper, we examine the detailed plasma discharge behavior and the structure characteristics of synthesized pPPy thin films grown by the APP polymerization technique relative to gas flow rate and input power. Our experimental results show that the change in the discharge characteristics from streamer-like to glow-like discharge would be easily controlled and the characteristics of synthesized pPPy thin films using proposed method could be improved with high deposition rate thanks to optimal discharge gas flow rate and input power.

2. Experiment

Figure 1 shows a schematic diagram of proposed APPJs device employed in this research. A bundle of three glass tubes was combined via powered electrode, which was copper tape and attached 10 mm from the end of the jet. Three glass tubes of bundle had inner diameter of 1.5 mm (D_i), outer diameter of 3 mm, and length of 13 cm, respectively. The additional glass tube, which had an inner diameter of 20 mm and length of 60 mm, constituted a nucleation region where the pyrrole monomers were decomposed by the Ar plasma and a recombination region where the decomposed monomers and radicals were polymerized and deposited. The PTFE bottom holder was installed at the jet end for controlling the jet flow in the nucleation region. The high purity Ar gas (99.999%) was used as the discharge gas for plasma generation and its flow rates from 700 to 1600 standard cubic centimeters per minute (sccm). Liquid pyrrole monomer (Sigma-Aldrich Co., St. Louis, Missouri, USA, $M_w = 67 \text{ g}\cdot\text{mol}^{-1}$) was vaporized by the Ar gas, with a flow rate of 130 sccm. A high voltage probe (Tektronix P6015A) and current probe (Pearson 4100) were connected between the power source via inverter circuit and the oscilloscope (LeCroy WaveRunner 64Xi) to measure the applied voltage and total current, respectively. The photo-sensor amplifier (Hamamatsu C6386-01) was used to analyze the plasma infrared (IR) emission in nucleation region. An optical emission spectrometer (OES, Ocean Optics USB-4000UV-VIS) was used to verify the diverse excited N_2 , Ar, He, and carbonaceous species. All photographs of the devices and plasma plumes were taken with a DSLR camera (Nikon D5300) with a Macro 1:1 lens (Tamron SP AF 90 mm F2.8 Di). The field emission scanning electron microscopy (FE-SEM, HITACHI SU8220) was used to analyze the surface image and morphology. Fourier transform infrared spectroscopy (FT-IR) of these polymers was measured by a Perkin-Elmer Frontier spectrometer between 400 and 4000 cm^{-1} .

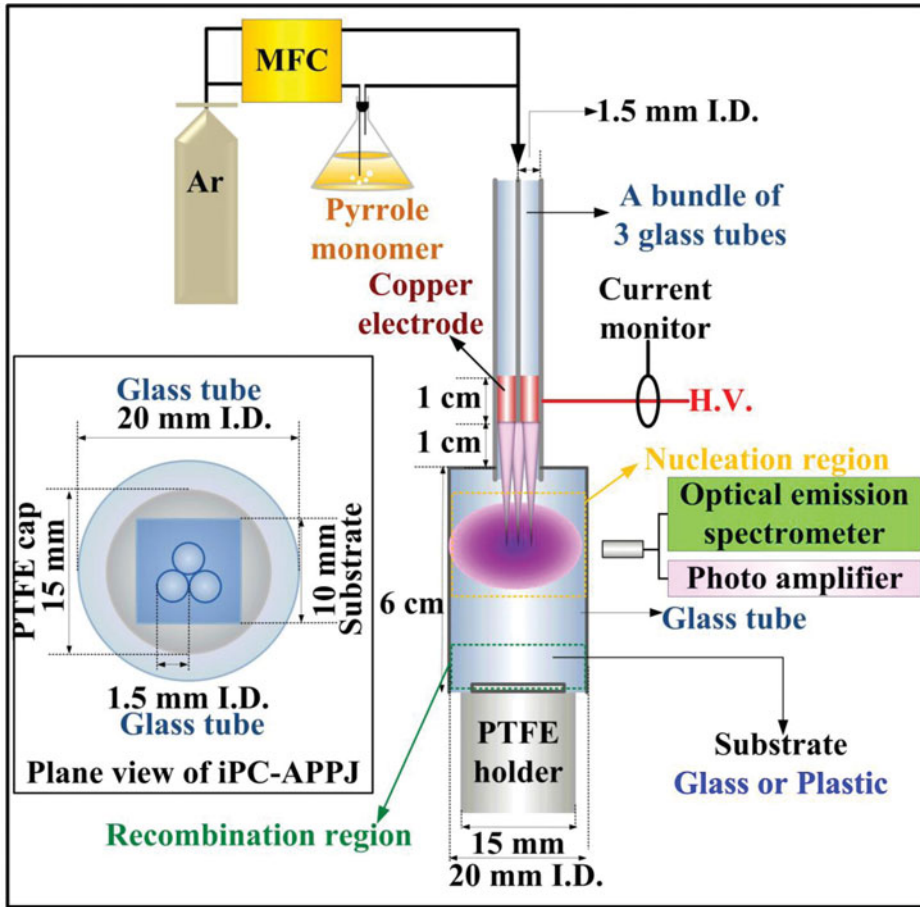


Figure 1. Schematic diagram of proposed atmospheric pressure plasma jets (APPJs) employed in this study.

3. Results and discussion

3.1. Experimental simulation and observation of optical, electrical and discharge characteristics under various conditions

Figure 2 shows the images of plasmas produced in nucleation region relative to the process parameters such as input powers and gas flow rates. In Fig. 2, the gas flow rates were changed from 700 to 1600 sccm, whereas peak values of input applied voltage were 7.5 kV for low input power and 12.5 kV for high input power. In order to understand the influence of the process parameters on the plasma discharge characteristics for the high quality plasma polymer films, the gas flow rates are varied from 700 to 1600 sccm under two different input power conditions: under the low input voltage of 7.5 kV, 700 sccm for case I, 1000 sccm for case II, 1300 sccm for case III, and 1600 sccm for case IV, in contrast, under the high input voltage of 12.5 kV, 700 sccm for case V, 1000 sccm for case VI, 1300 sccm for case VII, and 1600 sccm for case VIII.

As shown in Fig. 2(a), under the low voltage of 7.5 kV, the three individual plumes were observed to be produced despite the increase in the Ar gas flow rates from 700 to 1600 sccm, which would be like the streamer-like discharge shown in conventional plasma produced in

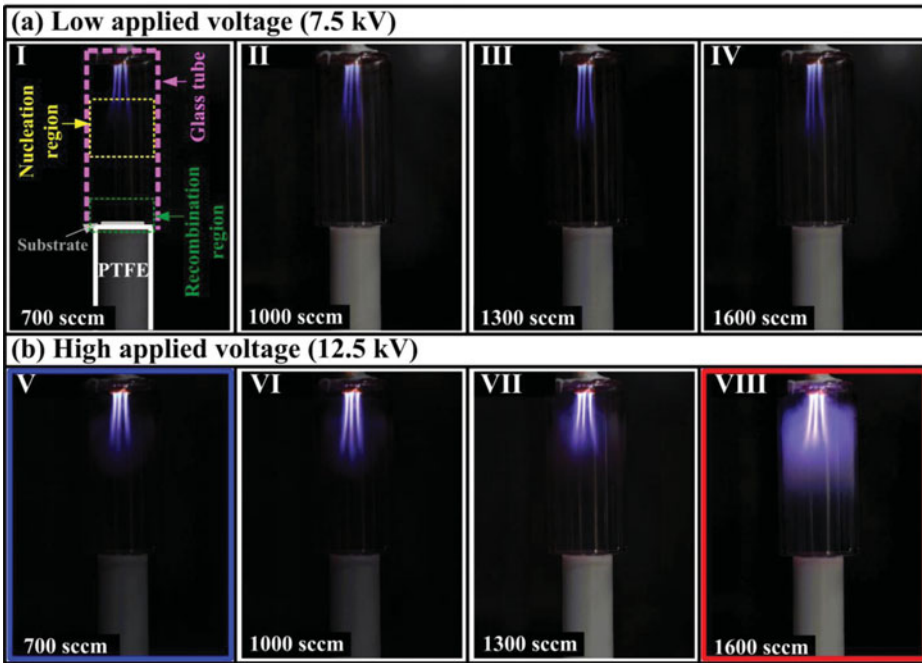


Figure 2. The plasma images of nucleation region in proposed APPJs as variations of input powers and gas flow rates (a) when the applied voltage is 7.5 kV and (b) when the applied voltage is 12.5 kV, respectively.

multi-array jets. On the other hand, when the input voltage was increased from 7.5 to 12.5 kV, the more strong and glow-like plasma with high intensities were clearly observed only when the Ar gas flow rate was 1600 sccm. This result confirms that the transition of the streamer-like discharge into the glow-like discharge depends strongly on the process parameter, especially the high Ar gas flow rate with a combination of the high applied input voltage in the proposed APPJ.

For the non-plasma flow numerical simulation shown Fig. 3, the four further simulation cases (Cases IX to XII) are supplemented to the experimental cases (Cases V to VIII) based on whether the PTFE bottom holder is located within or at the end of the glass tube. Figures 3(a) and (b) show the numerical results of secondary flow contours for x-z plane at $y/D_1 = -0.577$ and the distribution of secondary flow on the PTFE bottom holder for 8 Cases V to XII. In previous study, Case XI in Fig. 3 has shown the best performance to produce an intense and glow-like plasma condition as reported by Kim et al [13]. The intense and glow-like plasma could not be produced for Cases I to VII, in case that the PTFE bottom holder was located exactly at the end of the glass tube, implying that either the low input power case or the deficient gas flow rate condition could not satisfy the production of the intensified glow-like discharge. However, this experiment confirms that the high gas flow rate under high input power condition (Case VIII: Ar gas of 1600 sccm at an input voltage of 12.5 kV) enables the intense and glow-like discharge to be produced in nucleation region, as shown in Fig. 2(b). To get more comprehension for the plasma flow evolution via varying inflow conditions, various non-plasma flow simulations were employed. The numerical results of non-plasma condition had some limitation to depict the plasma flows, but it could provide important clues available for understanding the plasma flow behaviors. Thus, an analysis of the non plasma flow within the glass tube based on numerical computations was very meaningful. The numerical

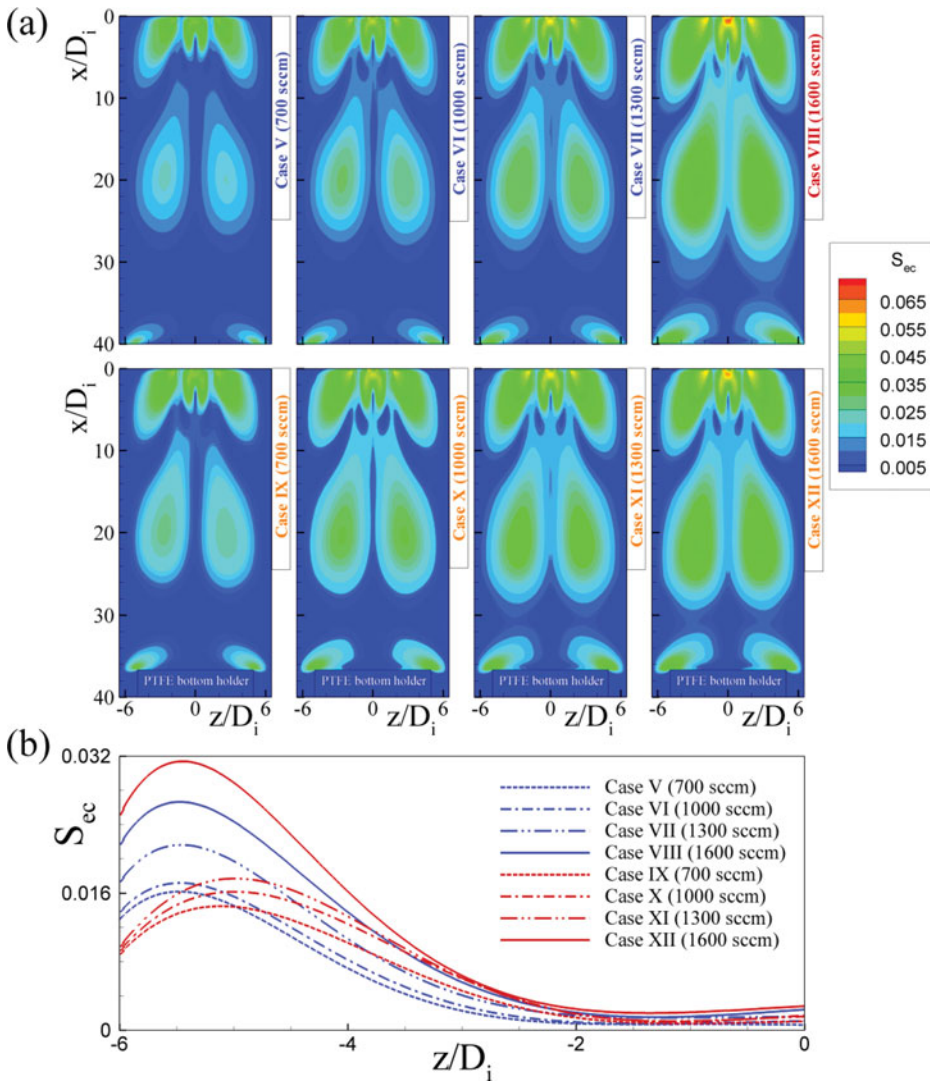


Figure 3. Comparison of (a) secondary flow contours for x-z plane at $y/D_i = -0.577$, and (b) distribution of secondary flow on the PTFE bottom holder for different Ar gas flow rates.

procedures and its validation were performed as the same way based on the previous study [13] and details of related discussions were not shown here for a simplification.

According to Kim et al. [13], the secondary flow motions were formed due to the sudden expansion of the glass tube, thus creating the recirculation flows within the glass tube. Such characteristic flow behaviors near the PTFE bottom holder were likely to play an important role in making intensified glow-like plasma. The mixing conditions between Ar gas stream in the vicinity of the PTFE bottom holder and newly incoming Ar gas flows were enhanced by secondary flows, thereby causing broad and intense glow-like plasma to be produced in a glass tube. In Figure 3, this flow behaviors were clearly observed and the S_{ec} was calculated by $S_{ec} = (V^2 + W^2)^{1/2} / U_c$ where V , W , and U_c denoted y - and z -direction velocity components, and center streamwise velocity of each plasma jet exit, respectively. As Ar gas flow rates increased, the secondary flows spatially expanded with increase in its value due to highly circulated flows. This feature was well matched with the experimental result of Fig. 2(b). In addition, near the

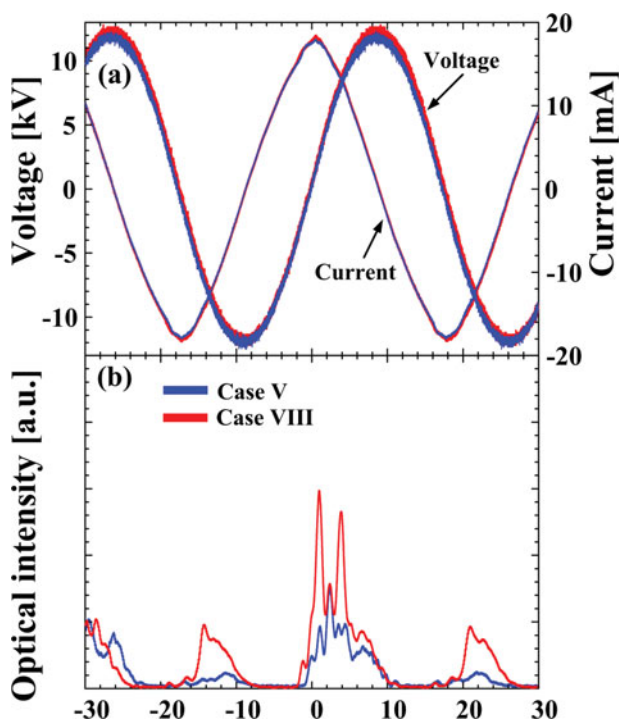


Figure 4. (a) The applied voltages, total currents, and (b) plasma infrared (IR) emission intensities measured in nucleation region in proposed APPJs for Case V and Case VIII, respectively.

PTFE bottom holder where the plasma polymerization process was mostly activated, the secondary flows became intense along the surface of PTFE bottom holder, and thus, more homogeneously discharged plasma condition for further complete plasma polymerization process could be induced, as described in Fig. 2. In particular, in Fig. 3(b), for the less inserted PTFE bottom holder with higher Ar gas flow rate (Case VIII), the distribution of secondary flow except the edge region was similar to that in the case of further inserted PTFE bottom holder with lower Ar gas flow rate (Case XI). This result confirmed that the variation of Ar gas flow rate was an effective parameter to control the plasma flows and its effect was more intensified coupling with the position of PTFE bottom holder. Consequently, in order to get a highly and widely discharged plasma condition for less inserted PTFE bottom holder case, an incoming Ar gas flow must contain higher momentum to strongly impinge the PTFE bottom holder for obtaining further provoked secondary flows.

Figures 4(a) and (b) show the applied voltages and related currents, and the resulting infrared (IR) emission intensities measured in nucleation region for two different Cases V and VIII. When comparing two cases, the input applied voltages are identical at 12.5 kV, whereas the gas flow rates between them are different, that is, 700 sccm for Case V and 1600 sccm for Case VIII. As shown in Fig. 4, more intense optical emissions were observed in nucleation region for high Ar gas flow rate, i.e., case VIII despite the same input applied voltage between Cases V and VIII, implying that the gas flow rate condition with a combination of the high input applied voltage can be a key parameter necessary for producing the intensified plasma that can decompose the pyrrole monomer in nucleation region. Unlike the case VIII, the high Ar gas flow rate of 1600 sccm under the low input applied voltage of 7.5 kV did not contribute to intensifying the IR emissions (not shown here).

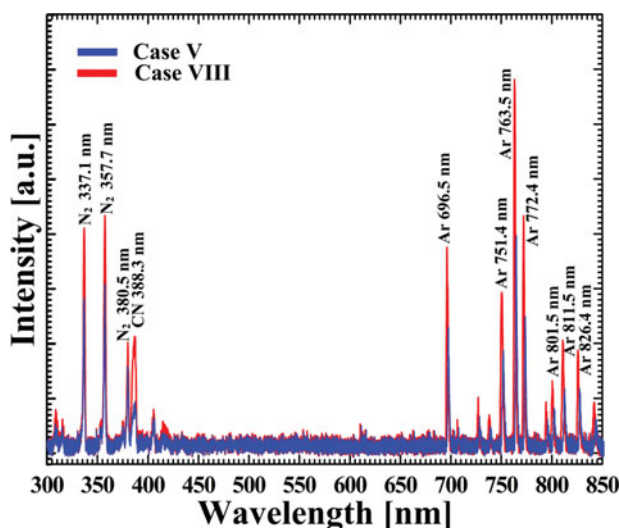


Figure 5. Optical emission spectra (OES) in region of wavelength ranging from 300 to 880 nm measured in nucleation region in proposed APPJs for Case V and Case VIII, respectively.

Figure 5 shows the optical emission spectra (OES) from 300 to 850 nm for Cases V and VIII in order to verify the excited N_2 , Ar, and carbonaceous species existing in plasma plume. As shown in spectrum measurements of Fig. 5, Ar (Ar: 695–850 nm), second positive system (SPS) (N_2 : 337, 357, and 380 nm), and carbonaceous (CN: 388 nm) peaks [14, 15] were clearly observed in both Cases V and VIII. The most-distinguishing feature of these results was that all OES peaks such as Ar, N_2 , and CN peaks were significantly increased in Case VIII despite the same input applied voltage between Cases V and VIII, as shown in Fig. 5. In general, reactive nitrogen species (RNS) are well-known to play an important role in various industrial applications and to be produced in more efficient, useful, and energy-dense plasma. In addition, in Case VIII, the CN ($B^2\Sigma \rightarrow X^2\Sigma$) peak, which was emitted during nucleation process of pyrrole monomer, was remarkably increased about by three times when compared with that of Case V. This means that the proposed APPJs can provide a sufficient fragmentation condition for pyrrole monomer in nucleation region and produce abundant radical species efficiently in recombination region of the pyrrole monomer.

3.2. Characterization of deposited pPPy thin film using APPJ

Figure 6 shows the scanning electron microscopy (SEM) images of pPPy thin film grown on glass substrates for 30 min. for two different Cases V and VIII. In Case V, the pPPy particles were hardly observed on the substrate presumably due to a weak plasma produced in nucleation region and the deposition rate was too low (only $14 \text{ nm}\cdot\text{min}^{-1}$). Whereas, in Case VIII, the polymer structures had many cross-linked networks and were hard bonded, and these structure characteristics would affect the flexibility and conductivity of polymerized thin film. The deposition rate was significantly increased by about $41 \text{ nm}\cdot\text{min}^{-1}$ under the room-temperature process.

Figure 7 shows the Fourier transform infrared spectroscopy (FT-IR) spectrum of pPPy thin film grown on plastic substrates for 60 min. for two different Cases V and VIII under the room-temperature process. FTIR spectrum was performed using the transmittance method since the pPPy films polymerized in this experiment were too thin to adopt the absorbance

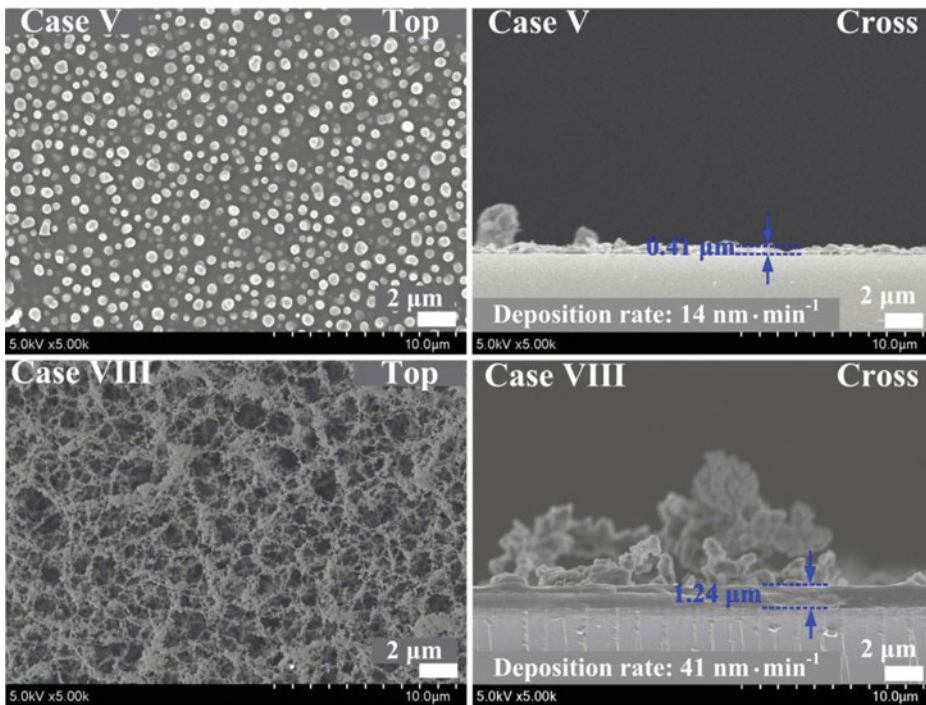


Figure 6. Top and cross-section views of scanning electron microscopy (SEM) images of plasma polymerized pyrrole (pPPy) nanoparticles thin film prepared via proposed APPJs after 30-min. on glass substrates for Case V and Case VIII, respectively.

method. As shown in spectrum measurements of Fig. 7, in Case VIII, the 3250 cm⁻¹ (N-H stretching), 2960 cm⁻¹ (aliphatic C-H stretching absorption) and 2215 cm⁻¹ (-C=H aliphatic vibration) peaks were more remarkably observed when compared with those in Case V. These peaks indicate that some parts of the polypyrrole were decomposed [16, 17]. From the viewpoint of conductivity, in Case VIII, the 2215 cm⁻¹ (-C=H aliphatic vibration), and

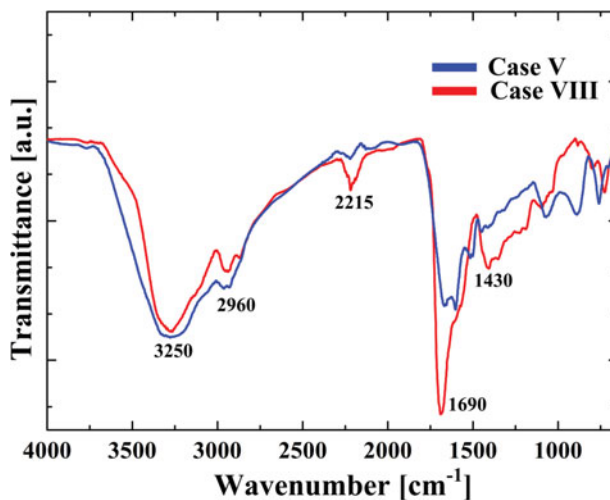


Figure 7. Overview Fourier transform infrared spectroscopy (FTIR) spectra of pPPy nanoparticles thin film prepared via proposed APPJs after 60-min. on plastic substrates for Case V and Case VIII, respectively.

1690 cm^{-1} (C=C double bond) peaks which have double bond obtaining π electrons, were significantly increased when compared with those in Case V [16–18]. Therefore, these related peaks guarantee the successful formation of pPPy films with good conductivity using halogen dopants [1, 19].

4. Conclusions

We have numerically and symmetrically examined the plasma discharge behavior and related structure characteristics of plasma-polymerized pyrrole (pPPy) thin films deposited by atmospheric pressure plasma (APP) polymerization technique relative to the gas flow rate and input power. The properties of synthesized pPPy films were improved as a result of adjusting the gas flow rates to 1600 sccm and input power to 12.5 kV during plasma polymerization. The deposition rate was also increased, thereby resulting in obtaining the high density and cross linking characteristics of the synthesized pPPy films. The electric conductivity will be improved by halogen (i.e., iodine) doping method. Accordingly, the adjustment of the process parameter during the pPPy film deposition using proposed APPJs technique can contribute to providing versatile advantages for future display technologies using flexible electrode-materials.

Funding

This work was supported by the National Research Foundation of Korea (NRF) grant funded by the Korea government (MSIP) (No. 2016R1C1B1011918).

References

- [1] Chiang, C. K., Fincher, C. R., Park, Y. W., Heeger, A. J., Shirakawa, H., Louis, E. J., Gau, S. C., & MacDiarmid, A. G. (1977). *Phys. Rev. Lett.*, 39, 1098.
- [2] Rahman, M. A., Kumar, P., Park, D.-S., & Shim, Y.-B. (2008). *Sensors*, 8, 118.
- [3] White, M. S., Kaltenbrunner, M., Głowacki, E. D., Gutnichenko, K., Kettlgruber, G., Graz, I., Aazou, S., Ulbricht, C., Egbe, D. A. M., Miron, M. C., Major, Z., Scharber, M. C., Sekitani, T., Someya, T., Bauer, S., & Sariciftci, N. S. (2013). *Nat. Photonics*, 7, 811.
- [4] Yoon, H., & Jang, J. (2009). *Adv. Funct. Mater.*, 19, 1567.
- [5] Kwon, S., Kim, W., Kim, H., Choi, S., & Park, B.-C., Kang, S.-H., & Choi, K. C. (2015). *Adv. Electron. Mater.*, 1, 1500103.
- [6] Burroughes, J. H., Bradley, D. D. C., Brown, A. R., Marks, R. N., Mackay, K., Friend, R. H., Burns, P. L., & Holmes, A. B. (1990). *Nature*, 347, 539.
- [7] Bárdos, L., & Baránková, H. (2010). *Thin Solid Films*, 518, 6705.
- [8] Uygun, A., Oksuz, L., Yavuz, A. G., Gule, A., & Sen, S. (2011). *Curr. Appl. Phys.*, 11, 250.
- [9] Miao, M., Chen, Q., Zhang, C., Cao, X., Zhou, W., Qiu, Q., & An, Z. (2013). *Macromol. Chem. Phys.*, 214, 1158.
- [10] Kim, D. H., Kim, H.-J., Park, C.-S., Shin, B. J., Seo, J. H., & Tae, H.-S. (2015). *AIP Adv.*, 5, 97137.
- [11] Park, C.-S., Kim, D. H., Shin, B. J., & Tae, H.-S. (2016). *Materials*, 9, 39.
- [12] Park, C.-S., Kim, D. H., Shin, B. J., Kim, D. Y., Lee, H.-K., & Tae, H.-S. (2016). *Materials*, 9, 812.
- [13] Kim, D. H., Park, C.-S., Kim, W. H., Shin, B. J., Hong, J. G., Park, T. S., Seo, J. H., & Tae, H.-S. (2017). *Phys. Plasmas*, 24, 023506.
- [14] Kim, J. Y., Ballato, J., & Kim, S. O. (2012). *Plasma Process. Polym.*, 9, 253.
- [15] Moon, S. Y., & Choe Spectrochim, W. (2003). *Acta - Part B At. Spectrosc.*, 58, 249.
- [16] Cruz, G. J., Olayo, M. G., López, O. G., Gómez, L. M., Morales, J., & Olayo, R. (2010). *Polymer*, 51, 4314.
- [17] Totolin, M., & Grigoraş, M. (2007). *Rev. Roum. Chim.*, 52, 999.
- [18] Wang, J., Neoh, K., & Kang, E. (2004). *Thin Solid Films*, 446, 205.
- [19] Gerard, M., Chaubey, A., & Malhotra, B. D. (2002). *Biosens. Bioelectron.*, 17, 345.